Laboratory Investigation (2014) 94, 692–702

Analysis of *MYB* oncogene in transformed adenoid cystic carcinomas reveals distinct pathways of tumor progression

Ana F Costa[1], Albina Altemani[1], Cristina García-Inclán[2], Florentino Fresno[3], Carlos Suárez[2], José L Llorente[2] and Mario Hermsen[2]

Adenoid cystic carcinomas can occasionally undergo dedifferentiation, a phenomenon also referred to as high-grade transformation. However, cases of adenoid cystic carcinomas have been described showing transformation to adenocarcinomas that are not poorly differentiated, indicating that high-grade transformation may not necessarily reflect a more advanced stage of tumor progression, but rather a transformation to another histological form, which may encompass a wide spectrum of carcinomas in terms of aggressiveness. The aim of this study was to gain more insight in the biology of this pathological phenomenon by means of genetic profiling of both histological components. Using microarray comparative genomic hybridization, we compared the genome-wide DNA copy-number changes of the conventional and transformed area of eight adenoid cystic carcinomas with high-grade transformation, comprising four with transformation into moderately differentiated adenocarcinomas and four into poorly differentiated carcinomas. In general, the poorly differentiated carcinoma cases showed a higher total number of copy-number changes than the moderately differentiated adenocarcinoma cases, and this correlated with a worse clinical course. Special attention was given to chromosomal translocation and protein expression of *MYB*, recently being considered to be an early and major oncogenic event in adenoid cystic carcinomas. Our data showed that the process of high-grade transformation is not always accompanied by an accumulation of genetic alterations; both conventional and transformed components harbored unique genetic alterations, which indicate a parallel progression. Our data further demonstrated that the *MYB/NFIB* translocation is not necessarily an early event or fundamental for the progression to adenoid cystic carcinoma with high-grade transformation.

Laboratory Investigation (2014) **94,** 692–702; doi:10.1038/labinvest.2014.59; published online 14 April 2014

KEYWORDS: adenoid cystic carcinoma; dedifferentiation; FISH; high-grade transformation; microarray CGH; *MYB*; NFIB

Adenoid cystic carcinoma with high-grade transformation (ACC-HGT) was first described as 'dedifferentiated' by Cheuk *et al* in 1999.[1] Subsequently, dedifferentiation in ACC has been recognized by several authors.[2–8] In 2007, Seethala *et al*[9] suggested the term 'high-grade transformation', and has since been adopted by many other authors, including for other salivary gland tumors, such as acinic cell and epithelial-myoepithelial carcinomas.[9–13] It was considered more appropriate from the fact that within the dedifferentiated component, the original line of epithelial differentiation may still be recognizable. However, our group recently described cases showing transformation to adenocarcinomas that are not poorly differentiated, that is, not 'high grade'.[14]

Irrespective of the exact terminology, it is clear that ACC-HGT is a clinicopathological entity distinct from classical ACC, showing evident morphological features such as focal or total loss of myoepithelial cell differentiation, marked nuclear enlargement, and squamous or micropapillary features in the transformed areas.[9] ACC-HGT has been shown to have higher Ki67 indexes and stronger p53 expression in the transformed component when compared with the conventional area.[15] Moreover, in contrast to

[1]Department of Pathology, University of Campinas/UNICAMP, Campinas, Brazil; [2]Department of Otolaryngology, IUOPA Hospital Universitario Central de Asturias, Oviedo, Spain and [3]Department of Pathology, Hospital Universitario Central de Asturias, Oviedo, Spain
Correspondence: Dr AF Costa, PhD, Departamento de Anatomia Patológica, Faculdade de Ciências Médicas, UNICAMP, Rua Tessália Vieira de Camargo 126, 13083-887 Campinas, São Paulo, Brazil.
E-mail: costa.anaflavia@gmail.com

Received 20 December 2013; revised 20 February 2014; accepted 6 March 2014

classical ACC, ACC-HGT appears to have an accelerated clinical course with a high propensity for lymph node metastases.[9,16] At the present moment, the combination of morphological criteria and Ki67 expression is still the most useful tool in identifying the transformed component in ACC-HGT.[12]

Few studies have been published on the molecular-genetic aberrations in ACC-HGT. Two genome-wide microarray CGH studies (one of which by our group) produced divergent results, probably because of the small series of tumors.[15] In 2011, Seethala *et al*[17] reported deletions in the conventional areas, whereas gains were found mostly in the transformed areas, mainly at 8q24, the location of *MYC*. Our own previous study revealed both gains and losses in the transformed area. The most frequent aberrations were gain of whole chromosome 8, and simultaneous gains at 6q23/loss at 9p22, possibly indicating the *MYB/NFIB* translocation. In addition, we found that a higher number of chromosomal aberrations was inversely correlated with the degree of gland differentiation, suggesting that high-grade transformation may not necessarily reflect a more advanced stage of tumor progression.[15] Similar to classical ACC, ACC-HGT carries few copy-number alterations or mutations.[15,17–19] Frierson and Moskaluk suggested that the neoplastic transformation may be driven by a limited number of changes in transcription regulatory genes, aggravated by changes in the chromatin structure.[20] Unfortunately, to date no studies have been done on transcriptional and epigenetic reprogramming in ACC-HGT.

The molecular mechanisms that trigger the morphologic transformation in salivary tumors still remain unclear. In the previous study carried out by our group, we analyzed only the transformed areas of a small number of ACC-HGT (four cases), using high-resolution microarray CGH.[15] In order to improve our understanding of the phenomenon of high-grade transformation in ACC, in the current study, we added four more cases and now both conventional and transformed components were analyzed for genome-wide copy-number aberrations by high-resolution microarray CGH, fluorescent *in situ* hybridization (FISH) and immunohistochemistry. Furthermore, special attention was given to chromosomal translocation and protein expression of *MYB*, which is currently being considered to be a major and early oncogenic event in classical ACC,[21–25] and which until now has not been studied in ACC-HGT. Our findings revealed genetic differences between the two components within each tumor, suggesting distinct pathways of tumor progression.

MATERIALS AND METHODS

Tissue Samples

Eight formalin-fixed and paraffin-embedded ACC-HGT were retrieved from the files of the Department of Pathology of the University of Campinas, Brazil and the Hospital Universitário Central de Asturias, Spain. Hematoxylin and eosin (H&E)-stained sections were reviewed to confirm the pathological diagnosis. The conventional area was graded on the basis of the predominant histological pattern as proposed by Szanto *et al*[26]: grade I (tubular and/or cribriform patterns); grade II ($<30\%$ of solid pattern) and grade III ($>30\%$ of solid pattern). The transformed area was identified according to the criteria described by Seethala *et al*,[9] and in all cases at least three of the major criteria were present: higher proliferation of tumor cells in the transformed area, at least a focal loss of myoepithelial cells surrounding tumor nests, nuclear size at least 2–3 times the size of classical ACC nuclei, thickened irregular nuclear membranes, and prominent nucleoli in a majority of cells. The study was approved by the local ethics committees.

In addition, based on the degree of gland differentiation, cellular pleomorphism, and mitotic activity, the transformed area was classified into: moderately differentiated adenocarcinomas (MDAs), when at least 2/3 exhibited gland differentiation (Figure 1a) and poorly differentiated carcinomas (PDCs), when gland differentiation was scarce or absent (Figure 1b).[27]

Immunohistochemistry

Sections of 5 μm from paraffin-embedded tissues were deparaffinized in xylene, rehydrated through a descending ethanol series, and submitted to heat-induced antigen retrieval in a water bath with Tris-EDTA pH 9.0 solution for 30 min. Subsequently, sections were immersed in 0.3% hydrogen peroxide in methanol and incubated with the primary antibody *MYB* (ab45150, Abcam, Cambridge, UK) and afterward with the EnVision peroxidase system, dual link (K4061, DAKOCytomation, Carpenteria, USA) for 1 h at 37 °C. The optimum antibody concentration was attained at 1:300 in dilution experiments using colon carcinoma as control tissue. After washing, sections were stained for 5 min at 37 °C with 3,3′-diaminobenzidine tetrahydrochloride and counter-stained with hematoxylin. Negative controls were run by omitting the primary antibody. For all tumors, three hotspot areas were chosen in conventional and in transformed components for counting of positive cells at $\times 40$ magnification using Imagelab analysis software (version 2.4, Softium informática LTDA-ME, São Paulo, Brasil). *MYB* expression was evaluated as the percentage of positive cells in relation to all tumor cells in these three areas in each sample.

DNA Extraction

Two cores of 5 mm of each paraffin-embedded tumor tissue block were collected; one from conventional and one from transformed areas for each case using a manual disposable biopsy punch (Kolplast LTDA, São Paulo, Brazil). The punch area was selected on the basis of H&E-stained slides.[28] Special care was taken to obtain high-quality DNA from the formaldehyde-fixed, paraffin-embedded tissues. DNA extracted from archival material can be partly degraded and cross-linked, the extent of which depends on the pH of the formaldehyde and the time of the fixation before paraffin

embedding. We applied an elaborate extraction protocol especially for paraffin-embedded tissues,[15] which includes thorough deparaffinization with xylene, methanol washings to remove all traces of the xylene, and a 24-h incubation in 1 mol/l sodium thiocyanate to reduce cross-links. Subsequently, the tissue pellet was digested for 3 days in lysis buffer with high doses of proteinase K (final concentration, 2 μg/μl, freshly added twice daily). Finally, DNA extraction was done by using the QIAamp DNA Mini Kit (Qiagen GmbH, Hilden, Germany).

Microarray CGH

Microarray CGH analysis was performed as described previously.[29] Reference DNA (extracted and pooled from blood of 18 different healthy female donors) and sample DNA were differently labeled by using the Enzo Genomic DNA Labeling kit according to the manufacturer's instructions (Enzo Life Sciences, Lörrach, Germany). Five hundred nanograms test and 500 ng pooled reference DNA were hybridized to a 180 k oligonucleotide array (SurePrint G3 Human CGH Microarray Kit 4 × 180 K, Agilent Technologies, Palo Alto, CA, USA). Hybridization and washing took place in a specialized hybridization chamber (Agilent Technologies). Images were acquired using a Microarray scanner G2505B (Agilent Technologies, Amstelveen, Netherlands). Analysis and data extraction were quantified using feature extraction software (version 9.1, Agilent Technologies). Normalization of the calculated ratios was done against the mode of the

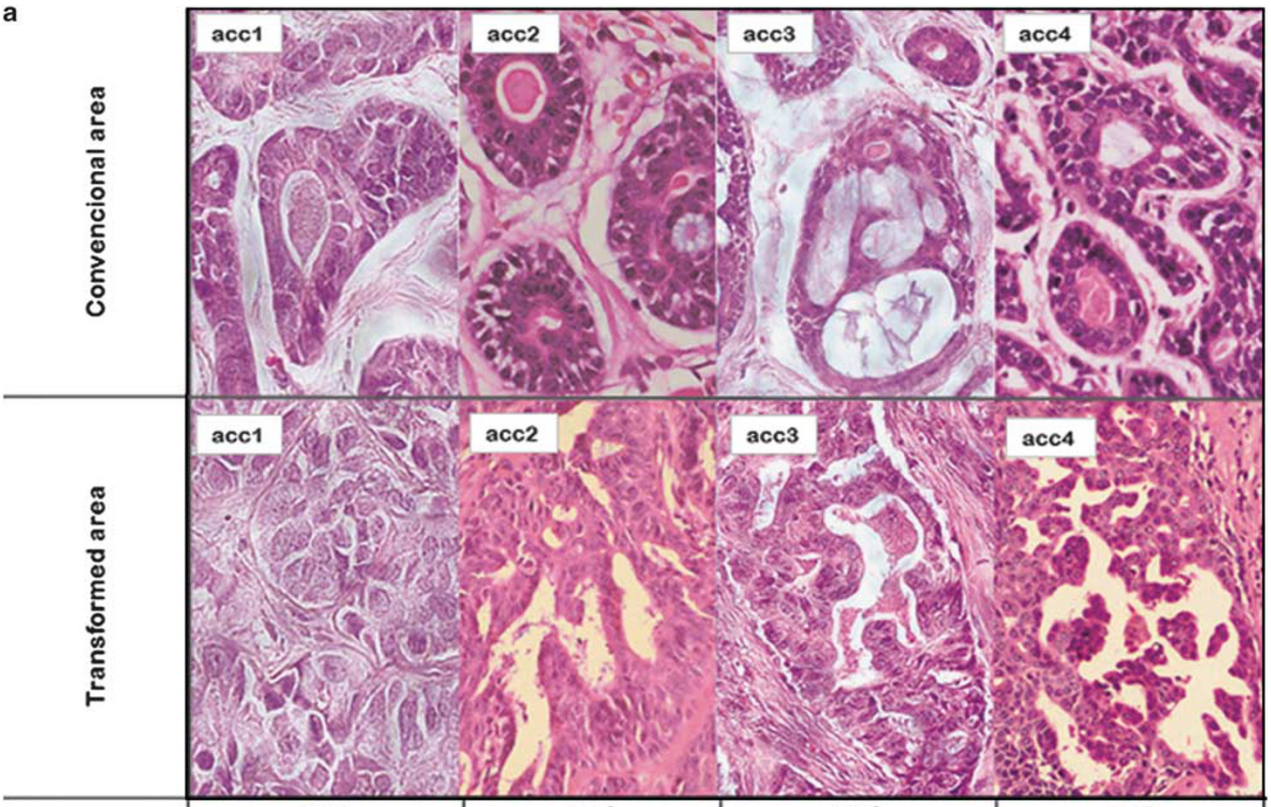

Case	acc1 losses	acc1 gains	acc2 losses	acc2 gains	acc3 losses	acc3 gains	acc4 losses	acc4 gains
CA (only)	No alterations		No alterations		No alterations		06q23_qter	09pter_p22
CA + TA (common)							04q13_q22	
TA (only)		4q12 6pter-qter 8pter-qter 21pter-qter		16pter_qter	06q23_qter	09pter_p22		

Figure 1 (**a**) Photomicrograph of representative H&E-stained paraffin sections of both conventional and transformed components of four cases of ACC-HGT with transformation to moderately differentiated adenocarcinoma (MDA). The lower panels show the unique and shared copy-number alterations of both components, as detected by microarray CGH. In red, 6q23/9p22 copy-number changes possibly indicating *MYB/NFIB* translocation. (**b**) Photomicrograph of representative H&E-stained paraffin sections of both conventional and transformed components of four cases of ACC-HGT with transformation to poorly differentiated carcinoma (PDC). The lower panels show the unique and shared copy-number alterations of both components, as detected by microarray CGH. In red, 6q23/9p22 copy-number changes possibly indicating *MYB/NFIB* translocation.

b

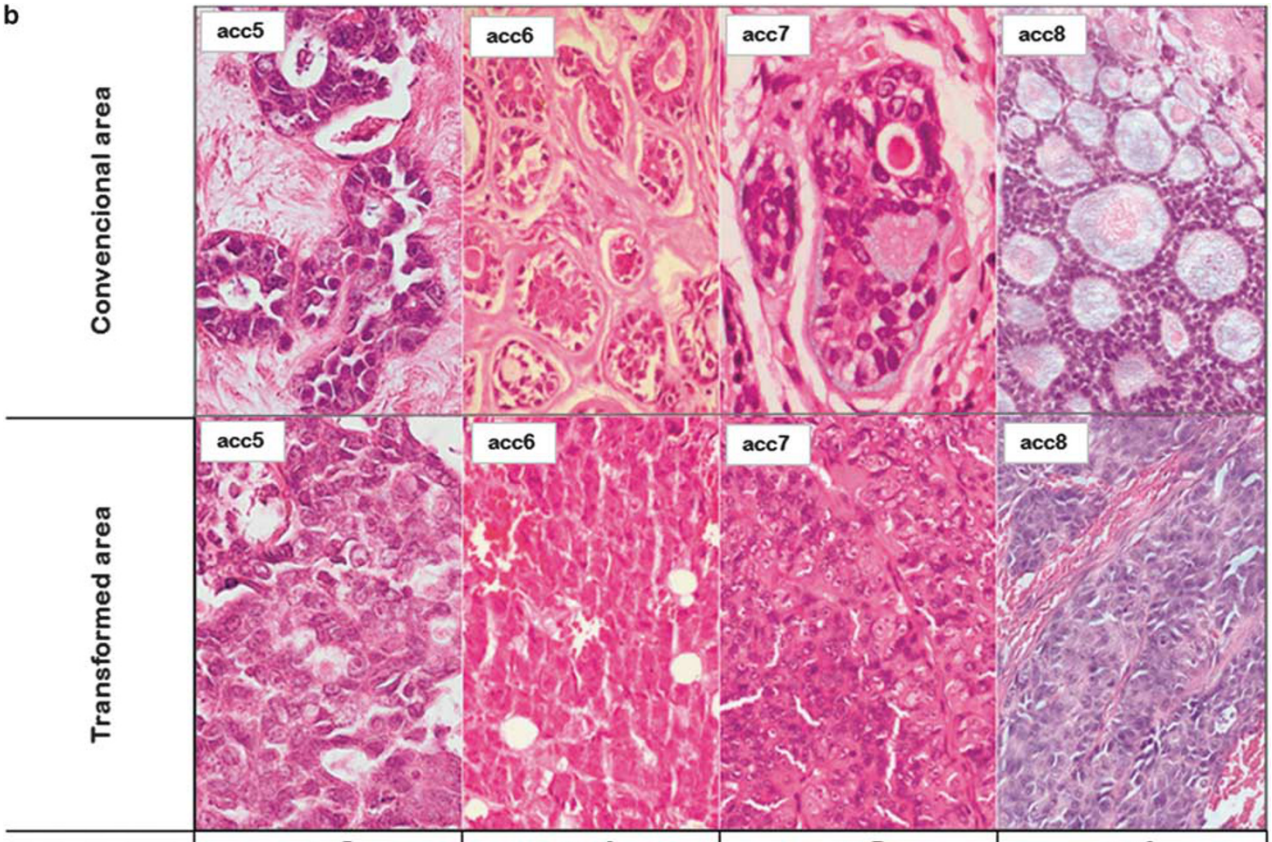

Case	acc5 losses	acc5 gains	acc6 losses	acc6 gains	acc7 losses	acc7 gains	acc8 losses	acc8 gains
CA (only)			No alterations				7q35 9pter_q12 10q26	
CA + TA (common)	06q23_qter 12q13	09pter_p22 08pter_qter 11q21				19pter_qter 22pter_qter	6q14 6q23_q23 6q25_qter 15q11 17p13 18q21 22q13 Xq21	6p22 6p21 8pter_qter 9p23
TA (only)			06q23_qter 09pter_p22 09p21_p13	06pter_q23 07pter_qter 08pter_qter 10q11_q11 18pter_qter 19pter_qter 20pter_qter	16q11_qter	1q12_ qter	1pter_36 1p36_35 2q13_37 14q21.3 15q12_15 15q15_q22 15q22 15q24_26 20pter_q13	1p36 1p35_q44 2p25_q13 6p21_q12 6q23 7pter_q35 7q35_qter 9q12_q34 11q13_q25 11q21 18p11_q21 18q21_qter 20q13_qter

Figure 1 Continued.

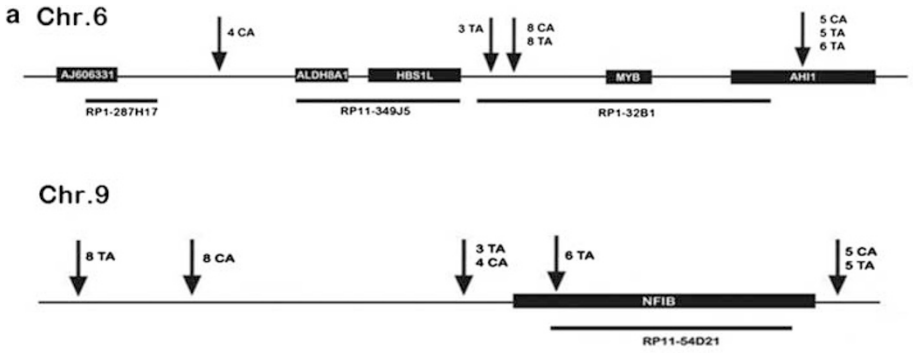

b Details of the probes and the putative breakpoints detected by microarray CGH

Cases	Area	Locus	Start (bp)	End (bp)	Size (bp)	Genes	BAC clones
Orange signal probes							
acc3	T	6q23.2-qter	135439476	170753165	35313690	MYB/AHI1	RP11-349J5
acc4	C	6q23.2-qter	135183041	170753165	35570125	MYB/AHI1	RP1-287H17
acc5	C	6q23.3-qter	135697914	170753165	35055252	AHI1	RP1-32B1
acc5	T	6q23.3-qter	135697914	170753165	35055252	AHI1	RP1-32B1
acc6	T	6q23.3-qter	135697914	170753165	35055252	AHI1	RP1-32B1
acc8	C	6q23.2-23.3	135078271	135471619	396634	near MYB	RP1-32B1
acc8	T	6q23.2-23.3	135078271	135471619	396634	near MYB	RP1-32B1
Green signal probe							
acc3	T	9pter-p22.3	0	14057337	14057337	near NFIB	RP11-54D21
acc4	C	9pter-p22.3	0	14057337	14057337	near NFIB	RP11-54D21
acc5	C	9pter-p22.3	0	14402208	14402208	NFIB	RP11-54D21
acc5	T	9pter-p22.3	0	14402208	14402208	NFIB	RP11-54D21
acc6	T	9pter-p22.3	0	14118789	14118789	NFIB	RP11-54D21
acc8	C	9p23	11148872	13562146	2413275	near NFIB	RP11-54D21
acc8	T	9p23	13096806	13378010	281205	near NFIB	RP11-54D21

bp - base pairs

Figure 2 (**a**) Schematic representation of the location of the *MYB* at chromosomal region 6q23, *NFIB* at chromosomal region 9p, and the BAC clones used for the FISH analysis. (**b**) Details on the localization of the BAC clones and the putative break points indicated by microarray CGH.

ratios of all autosomes. Graphics were plotted using a moving average of log 2 ratios of five neighboring clones. Gains and losses were defined as deviations of 0.2 or more from log 2 ratio = 0.0. High-level amplification was considered when at least two neighboring clones reached a log 2 ratio of 1.0 or higher. The locations of possible copy-number alterations were verified with the database of genomic variants and mapped according the human genome build NCBI 36 (http://projects.tcag.ca/variation/).

FISH

To identify *MYB/NFIB* rearrangements, FISH was performed on slides with 4-μm paraffin sections of ACC-HGT in both components using commercially available probes (BlueGnome, Cambridge, UK). On the basis of the putative break points detected in microarray CGH, we chose three different SpectrumGreen-labeled FISH probes on 6q23 near the *MYB* gene, and one SpectrumOrange-labeled FISH probe at 9p22 near the *NFIB* gene. Details of the probes and the putative break points detected by microarray CGH are given in Figure 2. Sections were deparaffinized in xylene, rehydrated in an ethanol series, and pretreated using the DAKO histology FISH accessory kit (DakoCytomation) in a water bath at 99 °C. After washing, sections were digested with pepsin for 10 min at 37 °C, and dehydrated in graded ethanol series. Simultaneous probe and slide denaturation was performed on a hot plate for 5 min at 82 °C, and hybridization took place at 45 °C overnight in a humidified chamber. Subsequently, the slides were washed in stringent solution for 10 min at 65 °C, dehydrated through a series of ethanol, and mounted in an antifade medium (Vectashield, Vector laboratories, Burlingame, USA) containing 4,6-dia-mino-2-phenylindole as a counterstain. The images were captured and processed using the Olympus BX61 fluorescence microscope and processed by Image J 1.43u software (Wayne Rasband National Institutes of Health, USA). We defined fusion positive when red and green signals from the 6q23 and 9p22 FISH probes colocalized in >20% of the total number of cells.

Statistical Analysis

All statistical procedures were performed using SPSS software for Windows, version 12.0 (SPSS, IL, USA). The Mann–Whitney *U*-test was used for comparison of the numeric variables between the groups as appropriate. For comparison of numeric variables between conventional and transformed areas of ACC-HGT, the Wilcoxon signed-rank test was used. All *P*-values were two-tailed and 95% confidence intervals were adopted. *P*-values <0.05 were considered significant.

RESULTS

Clinical Follow-up

The clinical and pathological data of this cohort are represented in Table 1. Four cases underwent transformation into

Table 1 Clinicopathological parameters of ACC-HGT

Cases	Age	Sex	Site	T	Treatment	Recurrences	Positive margins	Cervical lymph node metastasis	Distant Metastasis	Follow-up	Patient status	Grade	Histology		Glandular differentiation
													CA	*TA*	
acc1	44	F	Submandibular	T2	SE + RT	No	No	No	No	18	NA	I	T/C	MDA	Frequent
acc2	55	F	Palate	T4	SE + RT	No	No	No	No	154	NED	II	S	MDA	Frequent
acc3	65	M	Paranasal sinus	T4	SE + RT	No	No	No	No	8	DOC	III	S	MDA	Frequent
acc4	49	F	Parotid	T3	SE + RT	No	Yes	No	Yes (liver)	44	Alive	III	S	MDA	Frequent
acc5	61	F	Paranasal sinus	T4	SE + RT	Yes	NA	NA	No	144	NA	III	S	PDC	Scarce
acc6	64	F	Submandibular	T2	SE + RT	No	No	Yes	Yes (liver)	7	DOD	III	S	PDC	Scarce
acc7	58	F	Lip	T2	SE	No	No	No	No	25	NED	II	T/C	PDC	Scarce
acc8	47	M	Palate	T4	SE	No	No	No	Yes	19	NA	III	S	PDC	Scarce

Abbreviations: CA, conventional area; DOC, died of other causes; DOD, died of disease; F, female; M, male; MDA, moderately differentiated carcinoma; Mo, months; NA, not available; NED, no evidence of disease; PDC, poorly differentiated carcinoma; RT, radiotherapy; S, solid; SE, surgical excision; T, TNM classification; TA, transformed area; T/C, tubular/cribiform pattern.

MDA (cases acc1, acc2, acc3, and acc4) and four into PDC (cases acc5, acc6, acc7, and acc8). Median follow-up time was 52 months (7–154 months). The median age at presentation was 55 years (range 44–65 years), and six patients were female and two male. Two tumors occurred in the submandibular gland, two in the paranasal sinus, two in the palate, one in the parotid gland, and one in the lip. During follow-up, three patients developed metastasis and one patient local recurrence. Six patients received radiotherapy after resection.

DNA Copy-Number Analysis

Microarray CGH revealed copy-number alterations in all eight cases, of which four were in transformed area only and the other four cases were in both areas. The major recurrent gain was the whole chromosome 8. The most frequently amplified genomic region mapped to 9pter-p22/p23, encompassing *NFIB*. Other frequent events were the gain of whole chromosome 19 and at 11q21. The genomic region 6q23.3-qter, encompassing *MYB*, was the most frequent loss. Simultaneous 6q23.3-qter and 9pter-p22/p23 alterations, possibly indicating the *MYB/NFIB* translocation, occurred in five of eight cases (two MDA and three PDC): twice in both components, twice in the transformed area only and once in the conventional area only. In general, the PDC group showed a significantly higher total number of alterations than the MDA group (76 *vs* 11, respectively; $P = 0.017$, Mann–Whitney *U*-test), both in the conventional and transformed areas. Of the 76 alterations in the PDC group, 54 were in the transformed area and 22 in the conventional area. The MDA group showed a total of three alterations in the conventional area and eight in the transformed area. In both groups, gains were more frequent than losses.

Comparison of the genomic profiles of conventional and transformed areas revealed differences in the numbers of copy-number alterations, although not significant ($P = 0.061$, Wilcoxon test). Of a total of 47 gains in all eight cases, 37 were in the transformed and 10 in the conventional area. The transformed areas carried more losses than the conventional areas (25 *vs* 15, respectively) a total of 40 losses. One PDC case (acc5) showed an identical genetic profile in both components. In four cases (three MDA and one PDC), there were no genetic changes in the conventional area, but multiple abnormalities in the corresponding transformed component. In two cases (both PDC), the transformed area had the same genetic changes as its corresponding conventional area, plus additional aberrations. Finally, one case (MDA) showed one deletion shared by both components, whereas the conventional area carried additional aberrations. A detailed description of all copy-number alterations is given in Figure 1a and b.

MYB Translocation and Protein Expression

In five cases (acc3, acc4, acc5, acc6, and acc8), copy-number alterations involving a break point (the position where a gain

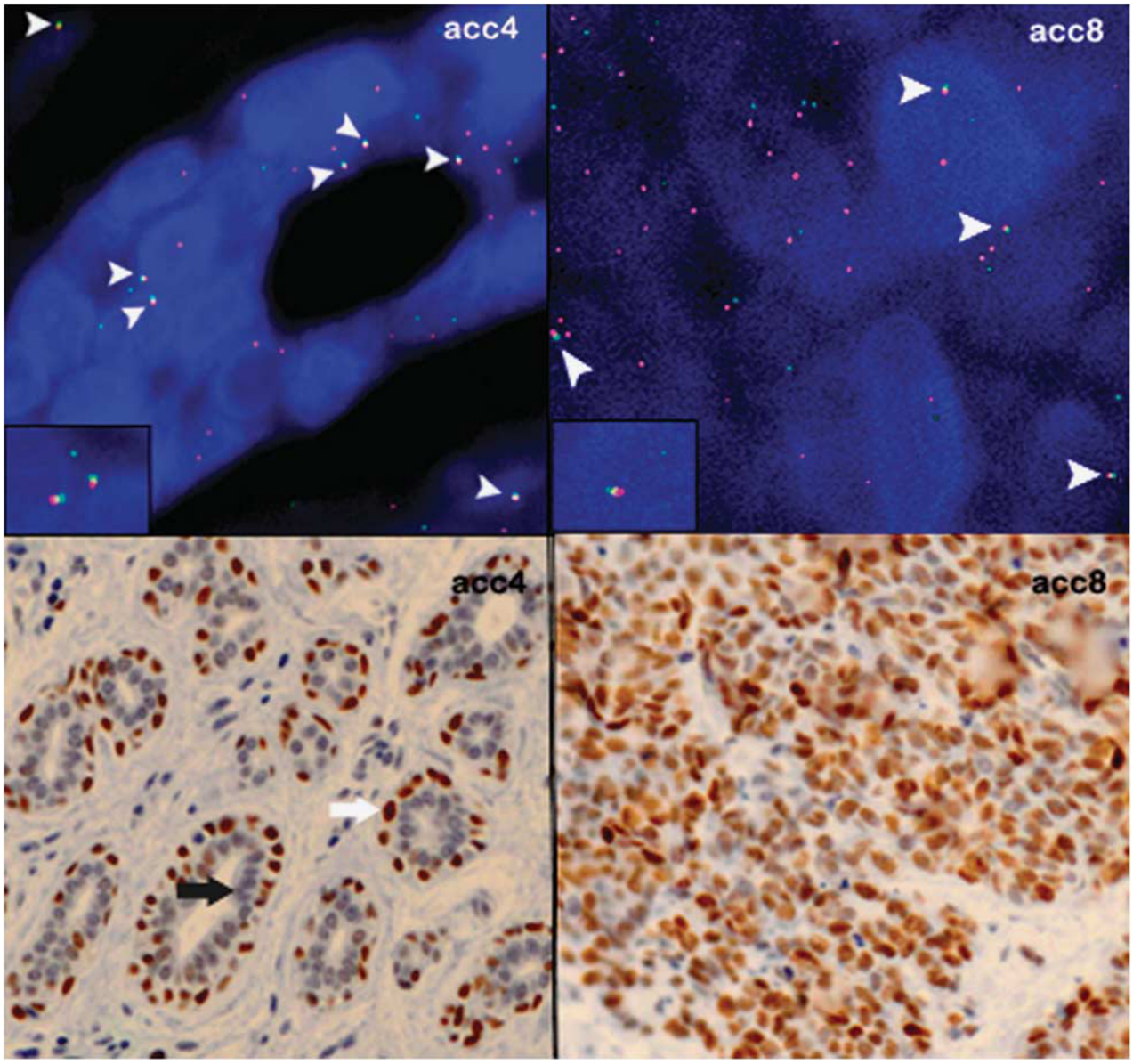

Figure 3 Two examples of *MYB/NFIB*-FISH and the corresponding protein expression of *MYB*. In the conventional area of acc4, the staining was entirely nuclear with strong expression in myoepithelial cells (indicated by the white arrow) and lack of expression in ductal cells (indicated by the black arrow). In the transformed area of acc8, the expression was observed only in ductal cells. Both cases showed the *MYB/NFIB* translocation (indicated by arrowheads). In the inset details of the approximation of green and red signals indicating *MYB/NFIB* translocation.

or a loss starts or ends) near 6q23 and 9p22 were observed simultaneously. In four cases this concerned a loss of 6q23-qter and a gain of 9pter-9p22, and in one case (acc6) there was a small deletion at 6q23 in combination with a deletion at 9p22 (Figure 1a and b). FISH was performed on these five cases to investigate whether this could indicate *MYB/NFIB* translocation. In two cases (acc3 and acc6), the break points were observed only in the transformed area: acc3 was fusion positive and acc6 was fusion negative. Cases acc5 and acc8 showed break points in both areas: only acc8 was fusion positive in conventional and transformed areas. In acc4, the break point was seen only in the conventional area and appeared fusion positive (Figure 3).

MYB was expressed in all eight cases of ACC-HGT, except for the transformed area of acc3. In the conventional areas, the staining was entirely nuclear with strong expression in myoepithelial cells and lack of expression in ductal cells (Figure 3). The transformed areas showed lower *MYB* expression than in the conventional area in five cases. High *MYB* expression in the transformed areas was observed in

Table 2 Analysis of *MYB* expression by immunohistochemistry (IHC), *MYB/NFIB* fusion by FISH, and copy-number alterations (CNA) at 6q and 9p by microarray CGH in ACC-HGT. Examples of MYB-IHC and *MYB/NFIB*-FISH of cases acc4 and acc8 (see asterisks) are given in Figure 3

	Conventional area			Transformed area		
Case	MYB index by IHC	MYB/NFIB by FISH	6q/9p by maCGH	MYB index by IHC	MYB/NFIB by FISH	6q/9p by maCGH
acc1	53.3	ND	No	43.3	ND	No
acc2	52.1	ND	No	66.9	ND	No
acc3	70.9	ND	No	0.0	Yes	Yes
acc4	69.4*	Yes*	Yes	53.0	ND	No
MDA (mean ± s.d.)	61.4 ± 10.07			40.8 ± 28.9		
acc5	67.2	No	Yes	67.0	No	Yes
acc6	72.3	ND	No	55.9	No	Yes
acc7	73.8	ND	No	68.5	ND	No
acc8	80.7	Yes	Yes	83.9*	Yes*	Yes
PDC (mean ± s.d.)	73.5 ± 5.5			68.8 ± 11.5		
MDA + PDC (mean ± s.d.)	67.4 ± 9.9			54.8 ± 25.2		

Abbreviations: maCGH, microarray CGH; MDA, moderately differentiated adenocarcinoma; ND, not done; PDC, poorly differentiated carcinoma.

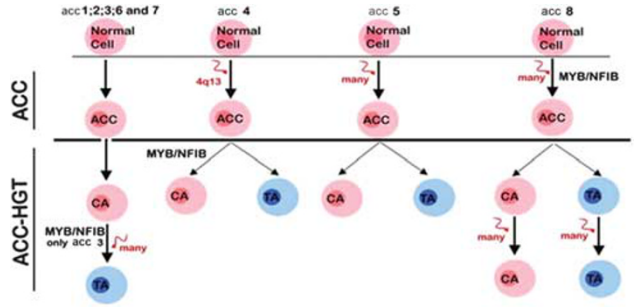

Figure 4 Schematic model of possible ways of ACC-HGT progression. Cases acc1,2,3,6, and 7 could be the result of a linear way of tumor progression, in which the transformed component derived from the conventional area by further acquisition of genetic abnormalities. Cases acc4,5, and 8 show both common and unique genetic changes that could be explained by a parallel way of tumor progression: case acc4 showed one common alteration in both components (4q13) and *MYB/NFIB* translocation in the conventional area only; case acc5 showed identical genetic changes in both components; case acc8 showed both common and unique copy-number changes in conventional and transformed areas. The common copy-number changes in both areas would have occurred early during the progression and before the split leading to the parallel progression.

ductal cells, and in myoepithelial cells *MYB* showed a focal expression pattern (Figure 3). However, the difference of *MYB* expression between conventional and transformed areas of ACC-HGT was not statistically significant ($P = 0.123$, Wilcoxon test). The results of the immunohistochemical expression and fusion analysis of *MYB* are summarized in Table 2.

Clinicopathological–Genetic Correlations

The complexity of the genomic profile of the tumor concurred with the clinical course of the patient. The four cases with transformation into MDA showed the lowest number of copy-number alterations. Among them, only acc4 showed liver and lung metastasis after 2 years. Case acc2 was a long-term survivor without recurrence or metastasis. Conversely, the PDC group showed a higher total number of alterations than the MDA group. Only acc7 showed a clinical course without recurrence or metastasis, although only a short-term follow-up (25 months) was available. Cases acc6 and acc8 showed the highest number of copy-number alterations and the worst clinical course. No differences in clinicopathological features were found between *MYB/NFIB* translocation-positive and negative cases or *MYB* expression. *MYB* expression was stronger in both conventional and transformed areas of PDC compared with MDA cases. However, only the difference between transformed areas of PDC and MDA groups was statistically significant (conventional area, $P = 0.083$ and transformed area, $P = 0.043$, Mann–Whitney *U*-test), Table 2.

DISCUSSION

The controversy regarding the terminology for dedifferentiation or high-grade transformation in ACC reflects the uncertainty about this phenomenon. Apart from ACC, an increasing number of salivary gland tumor types have been described as undergoing the high-grade transformation instead of dedifferentiation.[10–13] However, other tumors exhibiting this phenomenon, including liposarcomas,

neuroblastomas, and breast carcinomas, are still referred to as dedifferentiated.[30–32] Assuming that dedifferentiation implies the regression of a terminally differentiated cell to a less-differentiated stage within its own lineage,[33] then ACC dedifferentiation from a conventional to a high-grade transformed tumor would mean a next step in linear tumor progression. Therefore, we expected to find common genetic changes in conventional and transformed areas, and additional alterations in the transformed area. However, our results suggest that the high-grade component not always progresses directly from its conventional counterpart, and that the process of high-grade transformation can be the result of either linear or parallel progression. Our analysis of the genomic profiles of ACC-HGT indicated that five cases may have progressed from conventional toward transformed component by further acquisition of genetic abnormalities in the high-grade transformed area (acc1, acc2, acc3, acc6, and acc7). However, three cases (acc4, acc5, and acc8) showed genetic profiles that do not fit in this model of progression. They appear to have progressed clonally up to a certain point, substantiated by the observation of a number of identical copy-number alterations in both components. After this point, linear progression no longer explains the genetic events. Case acc5 showed identical genetic changes in both components, and similar findings have been reported studying dedifferentiated liposarcomas and biphasic carcinosarcomas.[34,35] In acc8, conventional and transformed areas demonstrated both common and unique copy-number changes, suggesting a parallel progression. Case acc4 showed one common alteration in both components, and two additional ones in the conventional area only. In this latter case, the genetic abnormalities that determine the high-grade transformation seem to have been acquired early in tumorigenesis or at least before the start of the phenotypic change (Figure 4).

A relevant question is which of the genetic alterations in ACC-HGT are early, tumor-initiating events and which alterations could be related to tumor progression and clinical behavior. It has been suggested that whole-chromosome copy-number changes could represent early events.[36] We found six of eight cases showing gain of whole chromosomes, such as 8, 19, 6, 7, 16, 18, 20, 21, and 22 (Figure 1a and b) in both components. However, a number of cases showed whole chromosome changes only in the transformed components (acc1, acc2, and acc6), which seem to suggest a late event in tumor progression.

The translocation t (6:9)(q22-23; p23-24) resulting in the fusion of the *MYB* oncogene with the transcription factor *NFIB*, has been considered an early and major oncogenic event in classical ACC.[21–25,37] However, in our series of ACC-HGT, it is clear that MYB/NFIB translocation is not always an initiating genetic event, given that in one case (acc3) the fusion was only detected in the areas of HGT and not in conventional areas. Second, our data suggest that high-grade transformation in ACC is not always a 'late' event, as our data show genetic divergence in several biphasic tumors, indicating that clinically significant lengths of time occurred between the divergence of conventional and transformed areas of tumors, allowing for somatic genetic divergence to occur in both components before coming to clinical attention and resection.

Our FISH analysis confirmed *MYB/NFIB* translocation in three of the five cases where microarray CGH analysis indicated simultaneous 6q22-23/9p22-23 copy-number changes (Table 2). Interestingly, in these three cases the break points were localized proximal to *MYB*, whereas the two translocation-negative cases had break points distal to *MYB,* within the gene *AHI1*. The translocation-positive cases acc3 and acc4 had terminal deletions 6q23-qter, whereas acc8 showed various copy-number levels along chromosome 6, including a small deletion located within band 6q23.3, proximal to *MYB* encompassing the genes *ALDH8A1* and *HBS1L* (Figure 1a and b). Most of the *MYB/NFIB* translocations described in the literature showed the break point within the *MYB* gene,[21,22] although break points close to, that is, outside *MYB* have also been reported.[37] Genomic imbalances involving 9p were seen in five cases. There were three cases (acc3, acc4, and acc5) with gains at the 9pter-p22.3 region, and acc8 had a small gain at 9p23 (Figure 1a and b). In acc6, the region 9pter-p22.3 was deleted as well as an additional small region at 9p21.3-p13.1. All five cases harbored either a normal 9pter copy number or a gain. This variability between the copy-number changes involving 9p is not uncommon in classical ACC and indicates that for 9p rearrangements, the preservation of the telomeric part of the *NFIB* is crucial.[38]

Expression of *MYB* in classical ACC has previously been shown to occur in both *MYB/NFIB* fusion-positive and -negative tumors.[23] Among our cases of ACC-HGT, only acc3 showed absence of *MYB* expression in the transformed area, despite being translocation-positive by FISH. High expression of *MYB* in classical ACC has been reported in tumors with translocation break points centromeric of *MYB,* similar to acc4 and acc8 in this study.[23,39] In contrast, acc5 and acc6 showed positive *MYB* expression and were translocation-negative. In the conventional areas, the staining was entirely nuclear, similar to reports on classical ACC, that is, strong expression in myoepithelial cells and lack of expression in ductal cells.[22,23,25] In the majority of our ACC-HGT cases, the transformed component showed lower *MYB* expression than in the conventional component, except for acc2 and acc8 (Table 2), possibly because there is partial or total loss of myoepithelial differentiation in the transformed area.[23] This suggests that in ACC-HGT other mechanisms of *MYB* activation may have a role, as has been demonstrated in colon and breast tumors.[40] In contrast to MYB/NFIB translocation, *MYB* expression could be considered an early event, because it is present in both areas of the tumor.

The correlation between the number of chromosomal aberrations and the degree of gland differentiation of the

transformed component in ACC-HGT was confirmed in this larger study.[15] PDC cases carried more complex genotypes, and in addition, they showed a more adverse clinical behavior. This finding supports the idea that classical ACC can undergo transformation into adenocarcinomas with variable degrees of differentiation, or even to other histological types,[41] which are not always high-grade, contributing to the controversy related to this phenomenon.

In conclusion, this study provided new insights in the tumor progression pathways of ACC-HGT by a pairwise comparison of genetic profiles of the conventional and transformed components, with emphasis on translocation *MYB/NFIB*. We have shown that the process of high-grade transformation is not always accompanied by an accumulation of genetic alterations; in some cases, both conventional and transformed components harbored unique genetic alterations, which indicate a parallel tumor progression. Our data further demonstrated that the *MYB/NFIB* translocation is not necessarily an early event or fundamental for the progression to ACC-HGT, as suggested previously in the literature for classical ACC.[21,22]

ACKNOWLEDGMENTS

Special thanks to: Bauke Ylstra and Paul Eijk, Microarray Laboratory, VU University Medical Center, Amsterdam, the Netherlands; Ana Claudia Piaza and Luzia Reis, Immunohistochemistry Laboratory, University of Campinas/Brazil; Sira Potes Ares, Department of Otolaryngology, IUOPA Hospital Universitario Central de Asturias Spain; Marta Alonso Guervós, Optical Microscopy and Image Processing Unit, Scientific-Technical Services, University of Oviedo, Oviedo, Spain. This work was supported in Brazil by FAPESP grants 2009/54377-2 and 2010/51571-0; CAPES (PDEE-BEX: 2275/11-2); supported in Spain by FIS (EMER07-048) and RTICC (RD12/0036/0015).

DISCLOSURE/CONFLICT OF INTEREST

The authors declare no conflict of interest.

1. Cheuk W, Chan JK, Ngan RK. Dedifferentiation in adenoid cystic carcinoma of salivary gland: an uncommon complication associated with an accelerated clinical course. Am J Surg Pathol 1999;23:465–472.
2. Moles MA, Avila IR, Archilla AR. Dedifferentiation occurring in adenoid cystic carcinoma of the tongue. Oral Surg Oral Med Oral Pathol Oral Radiol Endod 1999;88:177–180.
3. Chau Y, Hongyo T, Aozasa K, *et al.* Dedifferentiation of adenoid cystic carcinoma: report of a case implicating p53 gene mutation. Hum Pathol 2001;32:1403–1407.
4. Nagao T, Gaffey TA, Serizawa H, *et al.* Dedifferentiated adenoid cystic carcinoma: a clinicopathologic study of 6 cases. Mod Pathol 2003;16:1265–1272.
5. Ide F, Mishima K, Saito I. Small foci of high-grade carcinoma cells in adenoid cystic carcinoma represent an incipient phase of dedifferentiation. Histopathology 2003;43:604–606.
6. Brackrock S, Krüll A, Röser K, *et al.* Neutron therapy, prognostic factors and dedifferentiation of adenoid cystic carcinomas (ACC) of salivary glands. Anticancer Res 2005;25:1321–1326.
7. Hayashido Y, Yoshioka H, Tanaka N, *et al.* Dedifferentiation in adenoid cystic carcinoma of submaxillary gland: a case of report. Oral Oncol Extra 2005;41:84–88.
8. Sato K, Ueda Y, Sakurai A, *et al.* Adenoid cystic carcinoma of the maxillary sinus with gradual histologic transformation to high- grade adenocarcinoma: a comparative report with dedifferentiated carcinoma. Virchows Archiv 2006;448:204–208.
9. Seethala RR, Hunt JL, Baloch ZW, *et al.* Adenoid cystic carcinoma with high-grade transformation: a report of 11 cases and a review of the literature. Am J Surg Pathol 2007;31:1683–1694.
10. Skálová A, Sima R, Vanecek T, *et al.* Acinic cell carcinoma with high-grade transformation: a report of 9 cases with immunohistochemical study and analysis of TP53 and HER-2/neu genes. Am J Surg Pathol 2009;33:1137–1145.
11. Roy P, Bullock MJ, Perez-Ordoñez B, *et al.* Epithelial-myoepithelial carcinoma with high grade transformation. Am J Surg Pathol 2010;34:1258–1265.
12. Costa AF, Altemani A, Hermsen M. Current concepts on dedifferentiation/high-grade transformation in salivary gland tumors. Patholog Res Int 2011;17:1–9.
13. Nagao T. 'Dedifferentiation' and high-grade transformation in salivary gland carcinomas. Head Neck Pathol 2013;7(Suppl 1):S37–S47.
14. Bonfitto VL, Demasi AP, Costa AF, *et al.* High-grade transformation of adenoid cystic carcinomas: a study of the expression of GLUT1 glucose transporter and of mitochondrial antigen. J Clin Pathol 2010;63:615–619.
15. Costa AF, Altemani A, Vékony H, *et al.* Genetic profile of adenoid cystic carcinomas (ACC) with high-grade transformation versus solid type. Cell Oncol 2011;34:369–379.
16. El-Naggar AK, Huvos AG. Adenoid cystic carcinoma. In: Barnes L, Evenson JW, Reichart P, Sidransky D (eds World Health Organization Classification of Head and Neck Tumours, Lyon, 2005221–222.
17. Seethala RR, Cieply K, Barnes EL, *et al.* Progressive genetic alterations of adenoid cystic carcinoma with high-grade transformation. Arch Pathol Lab Med 2011;135:123–130.
18. Ho AS, Kannan K, Roy DM. The mutational landscape of adenoid cystic carcinoma. Nat Genet 2013;45:791–798.
19. Stephens PJ, Davies HR, Mitani Y, *et al.* Whole exoma sequencing of adenoid cystic carcinoma. J Clin Invest 2013;123:2965–2968.
20. Frierson Jr HF, Moskaluk CA. Mutation signature of adenoid cystic carcinoma: evidence for transcriptional and epigenetic reprogramming. J Clin Invest 2013;123:2783–2785.
21. Persson M, Andrén Y, Mark J, *et al.* Recurrent fusion of MYB and NFIB transcription factor genes in carcinomas of the breast and head and neck. Proc Natl Acad Sci USA 2009;106:18740–18744.
22. Mitani Y, Li J, Rao PH, *et al.* Comprehensive analysis of the MYB-NFIB gene fusion in salivary adenoid cystic carcinoma: incidence, variability, and clinicopathologic significance. Clin Cancer Res 2010;16:4722–4731.
23. West RB, Kong C, Clarke N, *et al.* MYB expression and translocation in adenoid cystic carcinomas and other salivary gland tumors with clinicopathologic correlation. Am J Surg Pathol 2011;35:92–99.
24. Fehr A, Kovács A, Löning T, *et al.* The MYB-NFIB gene fusion—a novel genetic link between adenoid cystic carcinoma and dermal cylindroma. J Pathol 2011;224:322–327.
25. Brill 2nd LB, Kanner WA, Fehr A, *et al.* Analysis of MYB expression and MYB-NFIB gene fusions in adenoid cystic carcinoma and other salivary neoplasms. Mod Pathol 2011;24:1169–1176.
26. Szanto MA, Luna ME, Tortoledo ME, *et al.* Histologic grading of adenoid cystic carcinoma of the salivary glands. Cancer 1984;54:1062–1069.
27. Wenning BM. Neoplasmas of the salivary glands. In: Wening BM, Heffess CS) (eds Atlas of head and neck pathology, China, 2008:628–631.
28. Prince ME, Ubell ML, Castro J, *et al.* Tissue-preserving approach to extracting DNA from paraffin-embedded specimens using tissue microarray technology. Head Neck 2007;29:465–471.
29. Buffart TE, Israelli D, Tijssen M, *et al.* Across array comparative genomic hybridization: a strategy to reduce reference channel hybridizations. Genes Chromosomes Cancer 2008;47:994–1004.
30. Helczynska K, Kronblad A, Jögi A, *et al.* Hypoxia promotes a dedifferentiated phenotype in ductal breast carcinoma in situ. Cancer Res 2003;63:1441–1444.
31. Coindre JM, Pédeutour F, Aurias A. Well-differentiated and dedifferentiated liposarcomas. Virchows Arch 2010;456:167–179.
32. Jögi A, Øra I, Nilsson H, *et al.* Hypoxia-induced differentiation in neuroblastoma cells. Cancer Lett 2003;197:145–150.
33. Jopling C, Boue S, Izpisua Belmonte JC. Dedifferentiation, transdifferentation and reprogramming: three routes to regeneration. Nat Rev Mol Cell Biol 2011;12:79–89.

34. Vécony H, Leemans CR, Ylstra B, *et al.* Salivary gland carcinosarcoma: oligonucleotide array CGH reveals similar genomic profiles in epithelial and mesenchymal components. Oral Oncol 2009;45:259–265.
35. Horvai AE, DeVries S, Roy R, *et al.* Similarity in genetic alterations between paired well-differentiated and dedifferentiated components of dedifferentiated liposarcoma. Mod Pathol 2009;22:1477–1488.
36. Ricke RM, van Ree JH, van Deursen JM. Whole chromosome instability and cancer:a complex relationship. Trends Genet 2008;24:457–466.
37. Mitani Y, Rao PH, Futreal PA, *et al.* Novel chromosomal rearrangements and break points at the t(6;9) in salivary adenoid cystic carcinoma: association with MYB-NFIB chimeric fusion, MYB expression, and clinical outcome. Clin Cancer Res 2011;17:7003–7014.
38. Persson M, Andrén Y, Moskaluk CA, *et al.* Clinically significant copy number alterations and complex rearrangements of MYB and NFIB in head and neck adenoid cystic carcinoma. Genes Chromosomes Cancer 2012;51:805–817.
39. Mukai HY, Motohashi H, Ohneda O, *et al.* Transgene insertion in proximity to the c-myb gene disrupts erythroid-megakaryocytic lineage bifurcation. Mol Cell Biol 2006;26:7953–7965.
40. Ramsay RG, Gonda TJ. MYB function in normal and cancer cells. Nat Rev Cancer 2008;8:523–534.
41. Altemani A, Costa AF, Montalli VA, *et al.* Signet-ring cell change in adenoid cystic carcinoma: a clinicopathological and immunohistochemical study of four cases. Histopathology 2013;62:531–542.